

4-Dimethylaminochalcone as a fluorescent probe: quantum chemical calculations of its interaction with the environment

S. K. Gularyan,^{a*} G. E. Dobretsov,^a B. M. Polyak,^a V. Yu. Svetlichny,^a
N. E. Zhukhlistova,^b B. M. Krasovitskii,^c L. I. Kormilova,^c and V. E. Zavodnik^d

^aResearch Institute of Physicochemical Medicine,
1a ul. Malaya Pirogovskaya, 119992 Moscow, Russian Federation.
Fax: +7 (495) 246 4512. E-mail: samvel_gularyan@mail.ru

^bA. V. Shubnikov Institute of Crystallography, Russian Academy of Sciences,
59 Leninsky prosp., 119333 Moscow, Russian Federation.
Fax: +7 (495) 135 1011

^cScientific and Technological Corporation "Institute for Single Crystals", National Academy of Sciences of Ukraine,
60 prosp. Lenina, 61001 Kharkov, Ukraine.
Fax: 380 (572) 332 0273

^dState Research Center of Russian Federation "Karpov Institute of Physical Chemistry",
10 ul. Vorontsovo Pole, 105064 Moscow, Russian Federation.
Fax: +7 (495) 975 2450

Ground-state RHF/6-311G(d,p) and density functional B3LYP/6-311G(d,p) quantum chemical calculations of 4-dimethylaminochalcone (DMAC), a sensitive fluorescent probe, were carried out for vacuum and for solvents of different polarity. The effect of the medium was included by the SCRF method in the framework of the polarization continuum model. The DMAC fragment comprising the aniline and propenone groups has a nearly planar conformation. The phenyl group can lie in the same plane or rotate by an angle within the limits of $\pm 20^\circ$ with a low barrier at 293 K. The results of calculations were confirmed by the data of X-ray study, according to which the phenyl group in the crystal is rotated by 20° . Calculations with allowance for solvation effects predict charge transfer from the dimethylamino group to the oxygen atom; the higher the medium polarity, the larger the degree of charge transfer (atomic charge of oxygen increases by 0.07 e in acetone). The calculated dipole moment of the DMAC molecule increases from 5.2 D (vacuum) to 5.9 D (heptane) and 6.9 D (acetone), which is in agreement with spectroscopic data. The energy of the DMAC–environment interaction was calculated. Due to large dipole moment of the DMAC molecule, the electrostatic component of this energy strongly depends on the environment polarity, which can be related to redistribution of the probe between the aqueous phase and cells and lipid structures of lipoproteins. The electronic absorption spectra of DMAC in solvents of different polarity were calculated; differences between the calculated and experimentally measured values are at most 15 nm.

Key words: fluorescent probe, 4-dimethylaminochalcone, quantum chemical calculations, ground state, X-ray analysis, polarity of the medium, solvation energy.

Fluorescent probes are widely used in studies of the structure and functions of biological objects¹ due to small size of the probe molecules and high sensitivity of the probe fluorescence to minor changes in the structures of the sites to which the probe is noncovalently bound. Therefore, probes act as indicators of structural changes in membranes, proteins, *etc.* Applications of fluorescent probes could be even more efficient provided that explanations for the mechanism of binding with biological objects and for the changes in the optical characteristics be available.

The aforesaid also concerns 4-dimethylaminochalcone (DMAC), one of the most sensitive fluorescent probes, which has been used in studies of proteins, biological membranes, and lipoproteins for more than three decades.^{1–4} First of all it should be noted that no explanation for high affinity of DMAC and similar probes to lipids is available so far. Indeed, at a lipid : water ratio of the order of 1 : 10000 almost all DMAC molecules are bound to the lipid.⁵ Because the DMAC molecules are located in the polar region of lipids,¹ their dipole moments can play a certain role. Additionally, the ground-

state dipole moment directly affects shifts in the absorption spectra depending on the medium polarity.^{6,7} Studies of the absorption spectra of DMAC in different solvents revealed large spectral shifts (up to 2000–3000 cm⁻¹) toward the low-frequency region upon an increase in the solvent polarity. A monotonic character of the experimentally observed spectral changes indicates an important role of nonspecific dipole-dipole interactions in solvation effects. Thus, spectroscopic data clearly indicate that changes in the electronic structure of the DMAC molecule under the action of the medium occur in the ground state.

In this connection we carried out quantum chemical calculations of the molecular geometry and dipole moment, and electronic absorption spectra of DMAC in solvents of different polarity that simulated the probe environment in lipid membranes and lipoproteins. An X-ray study of DMAC crystals was also performed.

Experimental and Calculation Procedure

The synthesis of DMAC was reported earlier.⁸ In this work we used diphenylhexatriene (Sigma) and organic solvents purchased from Aldrich.

Quantum chemical calculations were carried out on a workstation equipped with dual Opteron® processors using the Gaussian 03 Revision C.02 program (version for 64-bit operating system SUSE LINUX Pr. 9.1).⁹ Calculations with DMAC geometry optimization for vacuum and solvents were carried out by the restricted Hartree–Fock (RHF) method. The effect of the medium on the molecular structure of DMAC were included in the framework of the self-consistent reactive field (SCRF) method. The solvent properties were included in the framework of the polarization continuum model (PCM).^{10–13} The potential energy surfaces (PES) of the DMAC molecule were calculated for the following solvents: heptane, toluene, diethyl ether, THF, acetone, and water using the standard parameters of solvents and optimization criteria. The electronic absorption spectra of DMAC were calculated in the framework of the density functional theory (B3LYP approximation) with the 6-311G(d,p) basis set for isolated molecule and eight solvents, namely, cyclohexane, toluene, THF, acetone, acetonitrile, methanol, ethanol, and water.

DMAC single crystals were obtained by crystallization from toluene and acetone. The intensities of reflections were measured on a four-circle automated diffractometer Enraf-Nonius CAD-4, $\lambda(\text{Mo-K}\alpha) = 0.71073 \text{ \AA}$, β -filter, 293 K, $\theta/2\theta$ -scanning technique ($-15 \leq h \leq 14$, $-14 \leq k \leq 0$, $0 \leq l \leq 9$). The crystallographic characteristics of the DMAC crystals grown from toluene and the parameters of the X-ray experiment are listed in Table 1. The structure was solved by the direct method and refined anisotropically for the non-hydrogen atoms. Positions of all hydrogen atoms were located from the difference electron density syntheses and refined isotropically. All calculations were carried out using the SHELX97 program package.¹⁴ The bond lengths and bond angles calculated from the results of measurements are listed in Table 2.

Table 1. Crystallographic data and parameters of X-ray experiment for DMAC crystals grown from toluene*

Parameter	Value
Formula	C ₁₇ H ₁₇ NO
Molecular weight	251.32
Crystal system	Monoclinic
Space group	<i>P</i> 2 ₁ / <i>c</i>
<i>a</i> /Å	13.191(3)
<i>b</i> /Å	11.840(2)
<i>c</i> /Å	9.561(2)
β /deg	109.54
<i>V</i> /Å ³	1407.3
<i>Z</i>	4
<i>d</i> _{calc} /g cm ⁻³	1.186
μ /cm ⁻¹	0.73
Scanning range/deg	1.64–24.97
Number of measured reflections	2450
Number of refined parameters	241
<i>R</i> ₁ (<i>I</i> ≥ 2σ(<i>I</i>))	0.0346
<i>wR</i> ₂ (with respect to all reflections)	0.1083

* Yellow crystals of size 0.36×0.28×0.12 mm; crystals grown from acetone were of size 0.28×0.22×0.11 mm.

Table 2. Bond lengths (*d*), bond angles (ω), and dihedral angles (θ) in DMAC molecule obtained from Hartree–Fock (RHF/6-311G(d,p)) calculations for the ST point on the PES (see Fig. 1) and the results of X-ray study of DMAC crystals

Parameter	Calculations	X-ray (toluene)
Bond		
	<i>d</i> /Å	
C(1)–C(2)	1.332	1.323(3)
C(2)–C(3)	1.481	1.459(3)
C(3)–C(4)	1.503	1.476(3)
C(8)–C(9)	1.386	1.377(4)
C(9)–C(4)	1.390	1.360(4)
C(3)–O(10)	1.120	1.233(2)
C(1)–C(11)	1.464	1.456(3)
C(12)–C(13)	1.380	1.371(3)
C(18)–C(19)	1.375	1.370(3)
N(14)–C(17)	1.378	1.368(3)
N(14)–C(15)	1.449	1.441(3)
N(14)–C(16)	1.449	1.441(4)
Angle		
	ω /deg	
C(2)–C(1)–C(11)	128.2	129.6(2)
C(1)–C(2)–C(3)	120.1	122.2(2)
C(2)–C(3)–O(10)	121.8	120.3(2)
C(4)–C(3)–O(10)	119.5	119.4(2)
C(2)–C(3)–C(4)	118.7	120.3(2)
C(3)–C(4)–C(9)	123.0	122.7(2)
Angle		
	θ /deg	
C(2)–C(3)–C(4)–C(5)	160.4	161.2(2)
C(5)–C(4)–C(3)–O(10)	–18.9	–19.5(3)
O(10)–C(3)–C(2)–C(1)	–7.7	–1.0(3)
C(2)–C(1)–C(11)–C(19)	–3.0	–1.0(4)
C(16)–N(14)–C(17)–C(13)	13.3	2.8(4)

The DMAC partition coefficients (P) in the heptane–water and lipid–water systems were measured at 20 °C. A suspension of lipid membranes (in the form of liposomes) was prepared from egg phosphatidylcholine (Aldrich) by rapid injection of the lipid solution in ethanol into a buffer solution (0.15 M solution NaCl, 0.01 M solution of tris buffer, pH 7.4) using a known procedure¹⁵ followed by dialysis against the buffer solution over a period of 24 h.

The concentration of the lipid-bound DMAC was determined based on nonradiative energy transfer from duphenylhexatriene to DMAC as described earlier¹⁶ at a lipid concentration of 125 $\mu\text{mol L}^{-1}$ and probe concentrations in the range from 0.1 to 1 $\mu\text{mol L}^{-1}$.

Results and Discussion

Electronic structure of isolated DMAC molecule. Earlier, the DMAC molecule was assumed to have a planar ground-state geometry.¹⁷ Our calculations also predict the possibility for other, energetically more favorable, conformers to exist. Figure 1 shows a fragment of the PES of the DMAC molecule in the vicinity of a global potential energy minimum (point ST). The saddle points TS1 and TS2 correspond to nonplanar conformations with a rotated phenyl ring and pyramidalized Me groups. These conformations are the transition states between the planar conformation of the DMAC molecule corresponding to the point FL (see Fig. 1) and its conformation corresponding to the point ST. According to calculations for 293 K, the relative energy of the planar conformation is at most 0.4 kcal mol^{−1}, those of the transition states TS1 and TS2 being at most 0.2 kcal mol^{−1}. The small

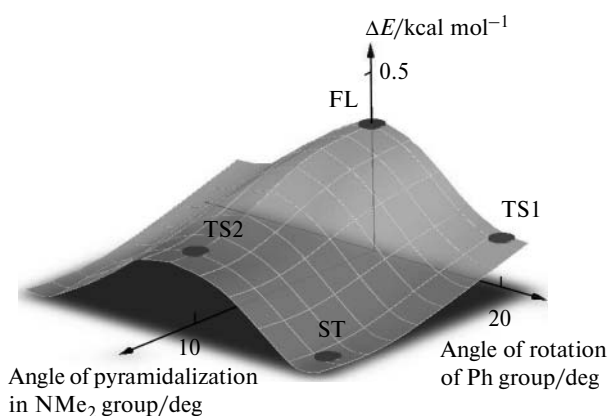
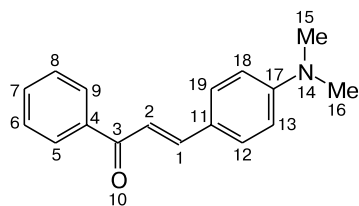


Fig. 1. Potential energy surface of isolated DMAC molecule in the vicinity of global energy minimum (ST). Obtained from RHF/6-311G(d,p) calculations (for notations TS1, TS2, and FL, see text).

energy differences allow all conformations of the DMAC molecule (see above) to be considered possible.

The parameters of the molecular structure (bond lengths, bond angles, and dihedral angles) at the potential energy minimum are listed in Table 2. The phenyl ring deviates by nearly 20° from the plane in which the propenone and aniline fragments lie and the NMe₂ group is characterized by rather high pyramidalization. The N(14)–C(17) bond length is 1.378 Å, being more similar to a double rather than single bond length.

The calculated dipole moment (μ_g) of isolated DMAC molecule is about 5.2 D. Traditionally, this type of fluorescent probe molecules is treated as comprised of electron-donating and electron-withdrawing groups responsible for the formation of the dipole moment.^{18–20} In our case these are the aniline fragment and the oxygen atom, respectively.

X-ray study. To confirm the results of quantum chemical calculations, we performed an X-ray study of the DMAC crystals grown from toluene and acetone. The results obtained appeared to be similar to the data reported by other authors who crystallized DMAC from another solvent (*cf.* data for the N(14)–C(17) bond length: 1.368 ± 0.003 (X-ray study) and 1.378 Å (calculated in this work) (see Table 2) vs. 1.372 Å (see Refs 21 and 22)). The calculated and experimental values of the dihedral angles are also similar. Additionally, the X-ray study confirmed the theoretically predicted rotation of the phenyl ring by 19°.

Effect of the medium on the electronic structure of DMAC molecule. Theory of solvation predicts an increase in the ground-state dipole moment of the solute molecule (μ_g) with an increase in the dielectric constant of the medium (ϵ).^{6,7} This also follows from the results of our quantum chemical calculations (Fig. 2), namely, $\mu_g(\text{DMAC}) = 5.2$ (vacuum), 5.9 (heptane), and

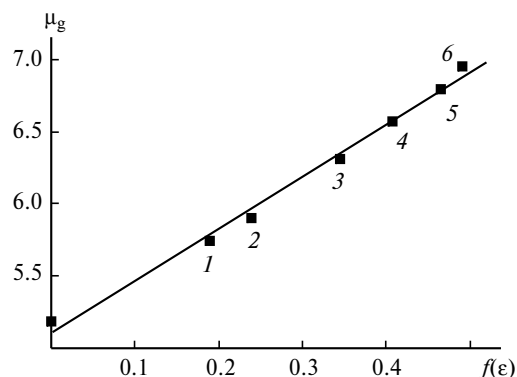


Fig. 2. Ground-state dipole moment (μ_g) of 4-dimethylaminochalcone molecule plotted vs. the medium polarity function ($f(\epsilon)$): heptane (1), toluene (2), Et₂O (3), THF (4), acetone (5), and water (6). Obtained from RHF/6-311G(d,p) calculations. The point in the ordinate axis corresponds to the dipole moment of isolated DMAC molecule.

6.9 D (acetone). A spectroscopic study²³ of DMAC showed that $\mu_g = 6.3 \pm 0.6$ D in nonpolar solvents (heptane, hexane, toluene) and increases to 7.0 ± 0.7 D in acetone. This is in good agreement with the results of quantum chemical calculations. The dipole moment μ_g increases linearly (see Fig. 2) with an increase in the medium polarity function

$$f(\epsilon) = (\epsilon - 1)/(2\epsilon + 1),$$

as is expected from the Onsager theory⁶.

Changes in the dipole moment are due to additional charge transfer within the DMAC molecule under the action of the polar environment. The charges on the skeletal atoms were calculated by the NBO method incorporated into the Gaussian 03 program. According to calculations, an increase in the solvent polarity is accompanied by a monotonic increase in the negative charge Δq of the O atom from -0.67 e (vacuum) to -0.74 e (acetone). Simultaneously, the positive charges of the ring carbon atoms increase in the aniline fragment and the charges of the C atoms in the Ph ring also slightly increase. Almost 85% of the charge additionally transferred to the O atom comes from the dimethylaniline fragment, the contribution of the Ph ring being $\sim 10\%$.

Charge transfer causes some changes in the molecular geometry (Fig. 3), namely, the double bonds O(10)—C(3) (curve 1) and C(1)—C(2) (curve 2) are lengthened, whereas the single bonds C(1)—C(11) and C(2)—C(3) (curve 4) are shortened. The N(14)—C(17) bond length decreases due to electron density transfer from the N atom to the ring (curve 3). In other words, in polar media the extent of transfer of the negative charge from the di-

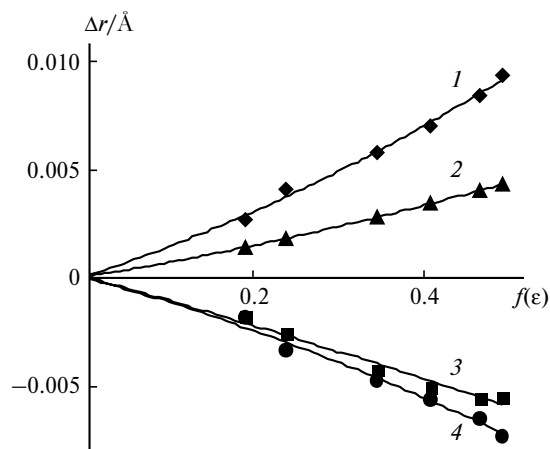


Fig. 3. Changes (Δr) in the bond lengths of C(3)—O(10) (1), C(1)—C(2) (2), N(14)—C(17) (3), and C(2)—C(3) (4) in the DMAC molecule plotted vs. the medium polarity function ($f(\epsilon)$). Circles in the curves correspond to the following order of solvents (from left to right): heptane, toluene, diethyl ether, THF, acetone, and water. Obtained from RHF/6-311G(d,p) calculations. The origin corresponds to isolated DMAC molecule.

methylamino group to the O atom increases, which leads to an increase in the dipole moment of the molecule.

Thus, changes in the medium polarity cause changes in the electronic structure of the DMAC molecule already in the ground state. The dielectric properties of the medium also lead to some deformation of the PES of the molecule (see Fig. 1). For instance, on going from vacuum to nonpolar solvents and then to acetone the relative energy of the transition state TS2 monotonically increases from 0.2 to 0.3 kcal mol⁻¹ and the relative energy of the transition state TS1 decreases by $\sim 25\%$.

Energy of the interaction of the DMAC molecule with the environment. The PCM model takes into account five components of the energy of nonspecific solvation. These are the energy of cavity formation in the solvent to house the probe molecule, the work of additional polarization and change in the molecular geometry of the probe on going from vacuum to the solvent, the energies of the probe—solvent electrostatic and dispersion interactions, and the repulsive energy.^{10–13,24,25} The results of B3LYP quantum chemical calculations of these energy components for DMAC are listed in Table 3. All of them depend on the properties of the medium. In particular, a change in the geometry and an increase in the dipole moment of the DMAC molecule in polar media require an energy expenditure of 3.3 kcal mol⁻¹ (for water). At the same time one can expect a gain in the electrostatic interaction energy upon transfer of DMAC to a medium of higher polarity. However, the energy expenditure for the formation of a cavity to house the probe in the interaction with water appears to be so high that the nonaqueous environment becomes more favorable.

Indeed, our measurements showed that the DMAC partition coefficient (P) in the heptane—water system is 300 ± 60 . Even more remarkable is the situation in the lipid—water system, namely, at a lipid : probe concentration ratio of $125 \mu\text{mol L}^{-1} : 3 \mu\text{mol L}^{-1}$ nearly 92% of DMAC molecules are bound to the lipid and only 8% remains in water ($P = (1.3 \pm 0.2) \cdot 10^5$). The parameter P is

Table 3. Energy of the interaction of DMAC and solvents of different polarity obtained from B3LYP/6-311G(d,p) calculations for $T = 293$ K

Interaction type	Energy/kcal mol ⁻¹		
	Heptane	Acetone	Water
Electrostatic	-4.1	-13.9	-15.9
Dispersion	-22.2	-20.7	-25.8
Repulsion	1.3	1.2	1.6
Formation of cavity	24.4	26.3	38.1
Polarization of DMAC molecule	0.3	2.7	3.3

Note. The energy of solvation calculated as the sum of the contributions of all interactions is -0.3 , -4.5 , and 1.4 kcal mol⁻¹ for heptane, acetone, and water, respectively.

related to the energy of transfer from one phase to another as follows²⁶

$$\Delta G = -RT \ln P.$$

For a bilayer of egg phosphatidylcholine one gets $\Delta G = -6.8$ kcal mol⁻¹. This is similar to the calculated difference between the solvation energies of DMAC in acetone and in water (-5.9 kcal mol⁻¹, see Table 3) but much higher than the difference between the solvation energies of DMAC in heptane and in water (-1.7 kcal mol⁻¹, see Table 3). Thus, the results of calculations suggest that in the lipid bilayer the DMAC molecule is situated in the region whose polarity is similar to that of acetone.²⁷ Spectroscopic data²⁸ and direct localization measurements²⁹ showed that DMAC molecules are mainly distributed within the layer of intermediate polarity between hydrophobic (heptane-like in polarity) chains and polar "heads" of the phospholipid.

Of course, the continuum model of the solvent can not correctly reproduce the molecular properties of such a complex and ordered structure, as the lipid membrane. Nevertheless, quantum chemical calculations have first pointed to a particular physical reason for the DMAC binding to the lipid bilayer, namely, to the region of intermediate polarity in the bilayer.

Effect of the medium on the absorption spectra of DMAC. The effect of the medium polarity on the position of maximum in the absorption spectrum can be assessed using the Lippert–Mataga relationship^{30,31} or semi-empirical theory.^{6,7} In both cases the molecules are for simplicity treated as spheres of some radius, the molecular dipoles are considered point dipoles located at the centers of the spheres, whereas the structural changes in the solute molecule under the action of the medium are

Table 4. Positions of maximum in the absorption spectrum of DMAC (λ_A) in media of different polarity according to experimental data²³ and results of B3LYP/6-311G(d,p) quantum chemical calculations* for the long-wavelength band in the electronic absorption spectrum

Medium	λ_A /nm	
	Experiment	Calculations
Vacuum	—	371
Cyclohexane	385	399
Toluene	398	412
Tetrahydrofuran	405	417
Acetone	407	419
Acetonitrile	415	427
Methanol	419	421
Ethanol	422	421
Water	427	429

* Calculated for the structure corresponding to the energy minimum (ST point in Fig. 1).

ignored. Quantum chemical calculations are free from these simplifications. The results of calculations of the electronic absorption spectra of DMAC (Table 4) are in good agreement with the experimental data.^{22,23} We calculated positions of the absorption bands corresponding to other possible conformations of the DMAC molecule at room temperature (see above) and found that this only leads to small variations in the position of the long-wavelength absorption band (at most 6 nm).

This work was financially supported by the Russian Foundation for Basic Research (Project Nos 05-04-49519 and 06-02-16943).

References

1. G. E. Dobretsov, *Fluorescentnye zondy v issledovanii kletok, membran i lipoproteinov* [Fluorescent Probes in Studies of Cells, Membranes, and Lipoproteins], Nauka, Moscow, 1989, 277 pp. (in Russian).
2. V. I. Sorokovoi, G. E. Dobretsov, V. A. Petrov, A. N. Nikitina, and Yu. A. Vladimirov, *Dokl. Akad. Nauk SSSR*, 1972, **205**, 500 [*Dokl. Chem.*, 1972 (Engl. Transl.)].
3. S. K. Gularyan, V. Yu. Svetlichny, and G. E. Dobretsov, *Membrane Cell Biol.*, 1997, **10**, 639.
4. S. K. Gularyan, V. Yu. Svetlichny, and G. E. Dobretsov, *Membrane Cell Biol.*, 1997, **11**, 401.
5. V. Yu. Svetlichny, G. E. Dobretsov, F. Merola, S. K. Gularyan, and T. I. Syreishchikova, *Biolog. Membr. [Biol. Membranes]*, 2006, **23**, 252 (in Russian).
6. N. G. Bakhshiev, *Opt. Zh.*, 2001, **68**, 26 [*J. Opt. Technol.*, 2001, **68** (Engl. Transl.)].
7. N. G. Bakhshiev, *Opt. Zh.*, 2001, **68**, 12 [*J. Opt. Technol.*, 2001, **68** (Engl. Transl.)].
8. S. V. Tsukerman, V. P. Maslennikova, and V. F. Lavrushin, *Opt. Spektrosk.*, 1967, **23**, 396 [*Optics Spectrosc.*, 1967, **23** (Engl. Transl.)].
9. M. J. Frisch, G. W. Trucks, H. B. Schlegel, G. E. Scuseria, M. A. Robb, J. R. Cheeseman, J. A. Montgomery, Jr., T. Vreven, K. N. Kudin, J. C. Burant, J. M. Millam, S. S. Iyengar, J. Tomasi, V. Barone, B. Mennucci, M. Cossi, G. Scalmani, N. Rega, G. A. Petersson, H. Nakatsuji, M. Hada, M. Ehara, K. Toyota, R. Fukuda, J. Hasegawa, M. Ishida, T. Nakajima, Y. Honda, O. Kitao, H. Nakai, M. Klene, X. Li, J. E. Knox, H. P. Hratchian, J. B. Cross, V. Bakken, C. Adamo, J. Jaramillo, R. Gomperts, R. E. Stratmann, O. Yazyev, A. J. Austin, R. Cammi, C. Pomelli, J. W. Ochterski, P. Y. Ayala, K. Morokuma, G. A. Voth, P. Salvador, J. J. Dannenberg, V. G. Zakrzewski, S. Dapprich, A. D. Daniels, M. C. Strain, O. Farkas, D. K. Malick, A. D. Rabuck, K. Raghavachari, J. B. Foresman, J. V. Ortiz, Q. Cui, A. G. Baboul, S. Clifford, J. Cioslowski, B. B. Stefanov, G. Liu, A. Liashenko, P. Piskorz, I. Komaromi, R. L. Martin, D. J. Fox, T. Keith, M. A. Al-Laham, C. Y. Peng, A. Nanayakkara, M. Challacombe, P. M. W. Gill, B. Johnson, W. Chen, M. W. Wong, C. Gonzalez, and J. A. Pople, *Gaussian 03, Revision C.02*, Gaussian, Inc., Wallingford (CT), 2004.

10. S. Miertus, E. Scrocco, and J. Tomasi, *Chem. Phys.*, 1981, **55**, 117.
11. S. Miertus and J. Tomasi, *Chem. Phys.*, 1982, **65**, 239.
12. F. Floris and J. Tomasi, *J. Comput. Chem.*, 1989, **10**, 616.
13. C. Amovilli and B. Mennucci, *J. Phys. Chem.*, 1997, **101B**, 1051.
14. G. M. Sheldrick, *SHELX97. Program for Crystal Structure Analysis (Release 97-2)*, University of Göttingen, Göttingen (Germany), 1997.
15. S. Batzry and E. D. Korn, *Biochim. Biophys. Acta*, 1973, **298**, 1015.
16. G. V. Belevich, G. Ya. Dubur, G. E. Dobretsov, N. K. Kurek, and M. M. Spirin, *Biolog. Membr.*, 1988, **5**, 768 [*Biol. Membr.*, 1988, **5** (Engl. Transl.)].
17. H. H. Szmant and A. J. Basso, *J. Am. Chem. Soc.*, 1952, **74**, 4397.
18. W. Rettig and M. Maus, in *Conformational Analysis of Molecules in Excited States*, Ed. J. Waluk, Wiley—VCH, New York, 2000, P. 1.
19. B. Boldrini, E. Cavalli, A. Painelli, and F. Terenziani, *J. Phys. Chem.*, 2002, **106**, 6286.
20. A. N. Nikitina, G. M. Fedyunina, B. Umirzakov, L. A. Yanovskaya, and V. F. Kucherov, *Opt. Spektrosk.*, 1973, **34**, 289 [*Optics Spectrosc.*, 1973, **34** (Engl. Transl.)].
21. T. Murafuji, Y. Sugihara, T. Morija, Y. Mikata, and S. Yano, *N. J. Chem.*, 1999, **23**, 683.
22. T. Murafuji, K. Sugimoto, S. Yanagimoto, T. Morija, Y. Sugihara, Y. Mikata, M. Kato, and S. Yano, *Heterocycles*, 2001, **54**, 929.
23. N. G. Bakhshiev, S. K. Gularyan, G. E. Dobretsov, A. Yu. Kirillova, and V. Yu. Svetlichny, *Opt. Spektrosk.*, 2006, **100**, 700 [*Optics Spectrosc.*, 2006, **100** (Engl. Transl.)].
24. H. Chuman, A. Mori, and H. Tanaka, *Anal. Sci.*, 2002, **18**, 1015.
25. I. Soteras, A. Morreale, J. M. Lopez, M. Orozco, and F. J. Luque, *Brazilian J. Phys.*, 2004, **34**, 48.
26. D. J. Giesen, G. D. Hawkins, D. A. Liotard, C. J. Cramer, and D. G. Truhlar, *Theor. Chem. Acc.*, 1997, **98**, 85.
27. R. G. Ashcroft, H. G. L. Coster, D. R. Laver, and J. R. Smith, *Biochim. Biophys. Acta*, 1983, **730**, 231.
28. G. E. Dobretsov, V. A. Petrov, V. E. Mishijev, G. I. Klebanov, and Yu. A. Vladimirov, *Studia Biophysica*, 1978, **71**, 181.
29. G. E. Dobretsov, N. K. Kurek, V. N. Machov, T. I. Syrejschchikova, and M. N. Yakimenko, *J. Biochem. Biophys. Methods*, 1989, **19**, 259.
30. E. Lippert, *Z. Naturforsch. A*, 1955, **10**, 541.
31. N. Mataga, Y. Kaifu, and M. Koizumi, *Bull. Chem. Soc. Jpn*, 1955, **28**, 690.

*Received July 7, 2005;
in revised form October 18, 2006*